35th Annual International Conference of the IEEE EMBS
Osaka, Japan, 3 - 7 July, 2013

Low-Voltage DEP Microsystem For Submicron Particle Manipulation In Artificial Cerebrospinal Fluid

Mohamed Amine Miled[1], *Student Member, IEEE*, and Mohamad Sawan[1], *Fellow, IEEE*

***Abstract*— In this paper, we present a new low voltage biochip for micro and nanoparticle separation. The proposed system is designed to detect the concentration of particles after being separated through reconfigurable DEP-based electrode architecture. The described system in this work is focusing on the particle frequency dependent separation. Experimental results in artificial cerebrospinal fluid (ACSF) show that each particle has its own crossover frequency. Thus based on the crossover frequency, particles are attracted to the electrode's surface, while others are pushed away. Five different particles are tested with different diameters in the range of 500 nm to 4 μm. All separation process is controlled by a CMOS chip fabricated using 0.18 μm technology from TSMC and powered with 3.3 V. Efficient particle separation is observed with low voltage, below 3.3V unlike other techniques in the range of kV. The proposed platform includes an advanced PDMS based assembly technique for fast testing and prototyping in addition to reconfigurable electrode architecture.**

I. Introduction

Several works proposed a compact lab-on-chip (LoC) and highlighted numerous aspects that have an impact on the LoC behavior. Xie et al. [1] proposed a system measuring the impedance of the air bubble requiring a special packaging care to avoid any interference on the measurements. In another contribution [2], a room-temperature microfluidic design was suggested based on a sequential plasma activation process. Moreover, Lee et al. [3] introduced a new packaging technique, known as Biolab-on-IC, based on magnetic field for individual magnetic bead manipulation, where the microfluidic architecture is mounted on top of the integrated circuit. However, in these techniques, systems still require external post processing or can be used only as an interface between the biological sample and any other control device. On the other side, Han and Frazier [4] discussed the reliability aspects of assembly and integration of microfluidic systems, by considering the system size, optical aspects, and connection parts. In all previously cited example, the power supply and used voltage or current are not considered as a limitation because the main goal is to prove the LoC concept.

The use of low voltage DEP is more attractive with the development of new microfabrication technologies which leads to smaller electrode space and size [5]. Then, it is possible to generate through low voltage signals a high electrical field, which induces the same DEP effect then when using conventional high voltage in the range of kV. The main advantage of such improvement is the design of fully integrated and automated LoC powered with small batteries to be implanted.

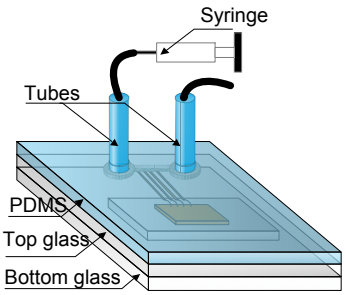

Fig. 1: System set-up using PDMS

The presented platform achieves a DEP separation with much lower voltage than other techniques [6], [7]. It has been tested with several microspheres with different charges, shapes in artificial cerebrospinal fluid to emulate the cortex environment.

In section II the proposed system is described and the main dielectrophoresis background is highlighted. The microfluidic structure and PDMS packaging process are also introduced, in addition to the microelectronic circuit. Experimental results are shown in Section III, with a discussion. Finally, a conclusion highlights the main contribution and results.

II. System Description

Tubing is a challenging step for a highly integrated system. The complexity is closely related to the very limited space to connect tubes to access holes. The diameter of the currently available commercial connectors is in the range of 6 mm; however, the distance between two adjacent access holes is 3 mm. Therefore, we used a tubing technique based on polydimethylsiloxane (PDMS) as shown in Fig. 1. which is more suitable for reusable system. For these purposes, the process described in this paper is particularly employed for a fast prototyping design.

First, the microstructure is cleaned using ethanol. Subsequently, the glass plate is heated to $80°C$, while the PDMS is polymerized and heated to $80°C$ also. Then, access holes are placed on the PDMS layer using biopsy punch, which is immediately stuck to the top glass of the microfluidic chip. The PDMS access holes have to be smaller than external tubes to apply small pressure and avoid liquid leakage when the inlet flow rate is not negligible. Even though, this technique is dedicated for low pressure applications, it can be extended to high pressure usage by adding a plasma

[1]A. Miled and M. Sawan are with Polystim Neurotechnologies Laboratory, Department of Electrical Engineering, Polytechnique Montréal, 2900 Édouard Montpetit, Montréal, Québec, Canada med-amine.miled at polymtl.ca

978-1-4577-0216-7/13/$26.00 ©2013 IEEE

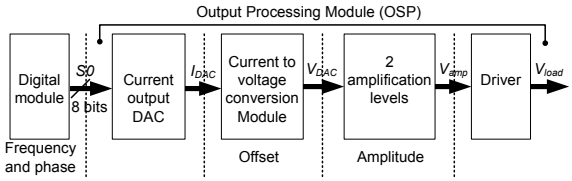

Fig. 2: Microelectronics circuit diagram

oxygen process to permanently seal the PDMS layer to glass. The interconnection system is tested with two different thicknesses, and the PDMS interconnection layer shows a good adherence up to 50 $\mu l/hour$ and 150 $\mu l/hour$ flow rate for 0.45 mm and 1 mm thicknesses, respectively.

The microfluidic architecture is designed for particle separation and detection using low voltage DEP [8] within a volume of 2 pl. The DEP effect is based on equations (1) and (**??**). Following the previously cited equation, both the voltage amplitude, frequency, and phase of applied signals affect DEP forces [8]. Equation (1) defines the dielectrophoretic force which is applied on the spherical particles.

$$\overrightarrow{F}_{sphere} = 2\pi a^3 Re\left(\frac{\epsilon_0 K_1^*(K_2 - K_1)}{2K_1 + K_2}\right)\nabla|E|^2 \qquad (1)$$

where K_1 and K_2 are the complex dielectric constants of the particle and the surrounding medium, respectively; K_1^* is the complex conjugate of K_1; ϵ_0 is the permittivity of air; E is the external electrical field; a is the radius of the spherical particle; ∇ is the differential vector operator; Re is the real part of the complex number. To reduce the amplitude of the applied voltages, an array of 10 μm × 10 μm electrodes is used. The channel length is 3 mm while its width is 650 μm. The microfluidic chip is composed of two 500 μm borofloat glasses. The microchannel is designed on the top glass layer, while the electrodes with a thickness of 200 nm are located on the bottom plate and connected to PCB pads by wire bonding. As the proposed LoC is designed for particle manipulation and detection, the microelectronic chip generates and controls the required electrical field. In fact, each L-shaped electrode generates an electrical field through dephased voltage signals by 180°C compared to the previous electrode. This way, particle manipulation depends on the shape and the weight of target particles in addition to the signal amplitude where particles with higher weight will be trapped due to the positive DEP effect. Thus, the microelectronic chip generates a variable amplitude sinusoidal wave and it dispatches signals in the microfluidic chip depending on the bioassay and application. Fig. 2 shows the detailed circuit implemented on a CMOS chip. To reduce power consumption, the digital module, DAC and current to voltage converter are powered with 1.8 V while buffer and amplification stages are powered with 3.3 V. To have a large sensing range the detection circuit is also powered with 3.3V.

III. Experimental Results

Fig. 3 illustrates the maximum pressure that can be supported by the PDMS based interconnectors in the case of

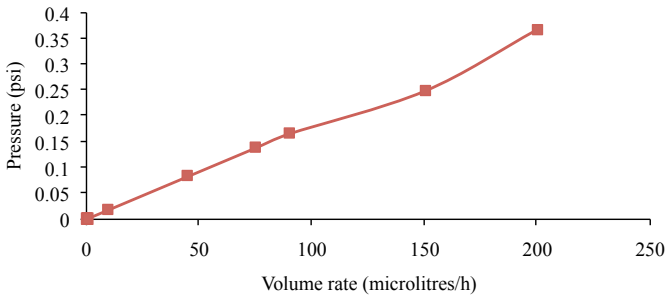

Fig. 3: ANSYS simulation results of the maximum pressure variation versus the volume rate of inlet liquid in a 50 μm microchannel depth

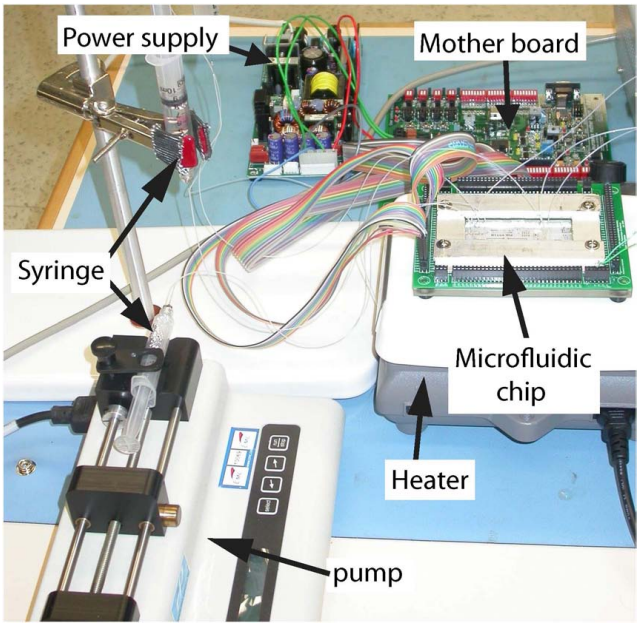

Fig. 4: System set-up photograph [9]

50 μm microchannel depth. The relationship between the pressure p and the volume rate V is linear, which is coherent with the modified Hagen-Poiseuille equation as stated by [10] and in equation 2. Based on this figure, a higher pressure can be applied when a thicker PDMS layer is placed, however this simulation does not take into account the adherence of the PDMS. Thus the simulation results were compared with experimental results to find the suitable thickness.

$$\Delta p = \frac{32\mu LV}{D^2} \qquad (2)$$

where D and L are the diameter and the length of the microchannel respectively, and μ is liquid viscosity. The system set-up shown in Fig. 4 to test the architecture is mainly composed of the microfluidic architecture, a syringe pump to inject ACSF, a CMOS chip and PCB-platform to generate the manipulation signals, the microfluidic chip which is fabricated through Lionix and a probe station PM5 from Cascade Microtech (some equipment are not shown in Fig. 4). As shown in Fig. 5, the epoxy is not practical to keep the microfluidic channel observable, and hence, the

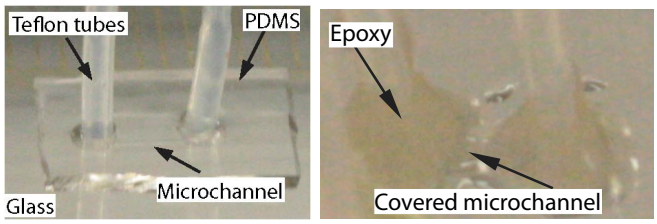

(a) (b)

Fig. 5: Proposed tubing process: (a) using temperature PDMS-based process, (b) using epoxy

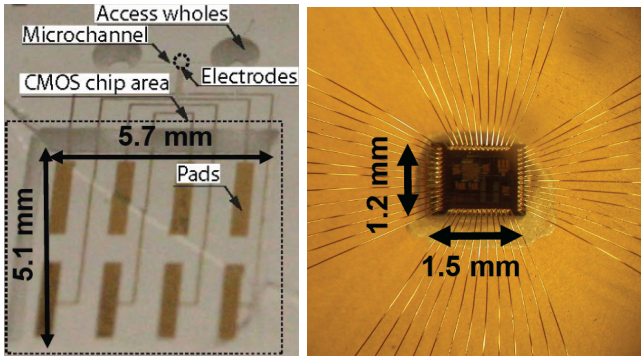

(a) (b)

Fig. 6: IC assembly: (a) microfluidic structure, and (b) microelectronics CMOS chip

PDMS-based packaging is used as presented in Fig. 5.

As described in Section II, the interconnection layer is fabricated with PDMS; however, another packaging is done using epoxy (731 from Epotek) as shown in Fig. 5. The epoxy is deposed manually on glass and kept at the room temperature for 24 h. The tubing process is achieved successfully and has a good adherence up to a volume rate of 150 $\mu l/h$.

The proposed packaging technique was tested with several PDMS thicknesses and sizes in order to find a sufficiently transparent and efficient packaging process for hybrid microelectronics/microfluidic microsystems as shown in Fig. 5. The size of designed PDMS layer is 6 mm $\times$ 6 mm and it is used to connect two access holes whose diameter is 1.5 mm. Furthermore the proposed method can be used with both epoxy or PDMS as shown in Fig. 5b. Different thicknesses of the PDMS are fabricated such as 0.45 mm, 1 mm and 1.75 mm. The best adherence is achieved, with thin PDMS layer with a thickness of 0.45 mm. The liquid flow rate is monitored through a Cole Parmer syringe pump. Both the 0.45 mm and 1 mm PDMS layers are tested with 50 μm channel depth. The PDMS-glass adherence is broken t 30 $\mu l/hour$ and 150 $\mu l/h$ flow rate for the 0.45 mm and 1 mm PDMS layer, respectively. Table I is a comparison with recently published results. As can be seen in the results presented in [11], similar designs of a reusable interconnector are presented. However, in [11] the PDMS layer is glued to the glass chip. To overcome this inconvenient, a thin PDMS based interconnector layer is used in our work. This method achieved good results for low pressure application, thus in [11], [12] and [13] the comparison is based on the pressure, but in our case, it was based on volume rate and pressure. To heat the glass substrate, we used a Corning PC-4200 heater. The CMOS chip is directly glued to the glass substrate using an epoxy H20E from Epotek.

A microelectronic chip is designed with TSMC 0.18 μm technology and is shown in Fig. 6. For practical reasons, the output signal from the CMOS chip is amplified to test the platform with different microsphere weights.

The biochip is tested with ACSF and microspheres to study the impact of brain environment on system architecture and microsphere behavior as shown in Fig. 7. First 400 μl of ACSF within 1.8 ml of DW with 40 μl of 1 μm microspheres are injected in the microchannel. An instant partial electrode failure is observed due to the high conductivity of the solution when an electrical field is applied. The DEP effect is ineffective when 20 $\%$ of the electrodes disappear.

However, the DEP effect is limited by the conductivity of the ACSF solution. The crossover frequency which corresponds to the transition from pDEP to nDEP is slightly affected if the ACSF concentration remains below 6 $\%$.

Efficient moving particle separation is achieved with a flow rate less than 20 nl/mn. A mixture of PS03N and PC05N polymer microspheres is achieved using square configuration of electrodes. At a frequency of 305 kHz, particles are trapped at the center of the electrode as shown in Fig. 8

The maximum applied voltage on electrodes is 6 V and 1.7 V using a PCB and IC based design respectively which is considerably lower compared to other techniques where the range of applied voltages is in kV.

However, a better frequency separation is observed with an efficient separation with U shaped electrodes as shown in Fig. 9. The selectivity in the proposed technique depends on

TABLE I: Main results summary and comparison

	Lee [13]	Gray [14]	Kua [15]	T.W.[1]	T.W.[2]
P. (psi)	75	315	30	0.07[3]	0.21[3]
V. R. ($\mu l/h$)	N.A.	N.A.	N.A.	30[4]	150[4]
Features	N.R.	H.P.	C.F.P.	R.	R.

P.: Pressure, V.R.: Volume rate, N.A.: Non Applicable, T.W: This work, H.P.: High Pressure, C.F.P.: Custom Fabrication Process, R.: Reusable, N.R.: Non Reusable [1] 0.45 mm PDMS thickness, [2] 1 mm PDMS thickness, [3] Simulation results, [4] Experimental results,

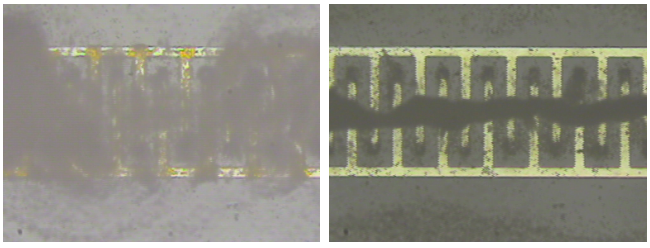

(a) (b)

Fig. 7: DEP effect through various concentration of ACSF: (a) shows nDEP when 5 μl,15 μl and 30 μl of ACSF are injected with 500 μl of DW respectively; (b) shows a pDEP effect for the same concentrations respectively

TABLE II: Experimental Minimum effective operation voltage threshold (MEOVT) for carboxyl-modified polystyrene beads versus electrode (E.) architecture (Arch.)

E. Arch.	Freq.	MEOVT $2.04\mu m$	$0.97\mu m$	$0.22\mu m$
U-shaped E.	200 kHz	1.7V	1.7V	1.7V
Octagonal E.	1.3 MHz	6V	12V	13V
SSM E.	200 kHz	1.7V	2.5V	6V

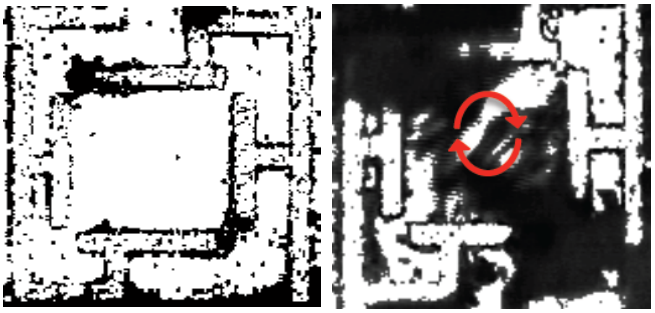

(a) (b)

Fig. 8: (a) Square shape electrode configuration before experiments, and (b) Mixing of PS03N and PC05N microspheres

frequency and particle shape and/or charge. The proposed technique can achieve a high selective separation with U-shape electrodes while using a buffer solution of 500 μl of D.W where the 25 μl of ACSF is injected and mixed with particles. In another side, the presented platform achieved a DEP separation with much lower voltage than other techniques as shown in table II.

IV. Conclusion

We have presented in this paper a new low-voltage LoC for micro-particle separation using DEP and tested with ACSF. Limitations regarding the electrode design were highlighted due to the high conductivity of the ACSF. However, low-voltage DEP separation was observed in ACSF and separation process based on the crossover frequency was successfully achieved in the same condition. The advantage of using low-voltage DEP is to reduce the power consumption of the device for a bioimplanted and developing an automated separation and detection process.

Acknowledgment

The authors acknowledge the financial support from NSERC and Canada Research Chair in Smart Medical Devices, and are grateful for the design and simulation tools supplied by CMC Microsystems.

References

[1] L. Xie, C. Premachandran, M. Chew, and S. C. Chong, "Development of a disposable bio-microfluidic package with reagents self-contained reservoirs and micro-valves for a dna lab-on-a-chip (loc) application," *IEEE Trans. Adv. Packag.*, vol. 32, no. 2, pp. 528–535, May 2009.

[2] M. Howlader, S. Suehara, H. Takagi, T. Kim, R. Maeda, and T. Suga, "Room-temperature microfluidics packaging using sequential plasma activation process," *IEEE Trans. Adv. Packag.*, vol. 29, no. 3, pp. 448–456, Aug. 2006.

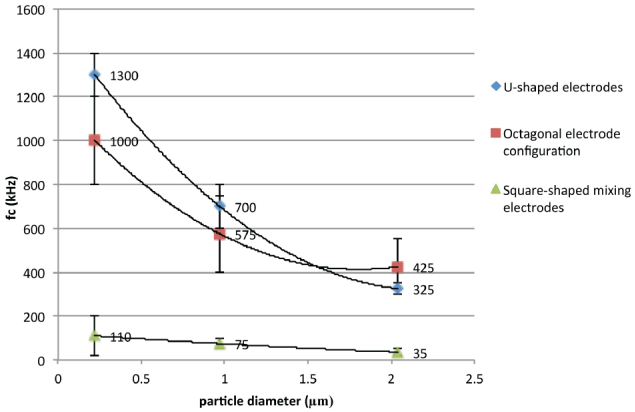

Fig. 9: crossover frequency (f_c) as a function of particle diameter for each implemented electrode architecture [16].

[3] H. Lee, Y. Liu, R. Westervelt, and D. Ham, "Ic/microfluidic hybrid system for magnetic manipulation of biological cells," *IEEE J. Solid-State Circuits*, vol. 41, no. 6, pp. 1471–1480, Jun. 2006.

[4] K.-H. Han and A. Frazier, "Reliability aspects of packaging and integration technology for microfluidic systems," *IEEE Trans. Dev. Mat. Rel.*, vol. 5, no. 3, pp. 452–457, Sep. 2005.

[5] S. Hwang, C. LaFratta, V. Agarwal, X. Yu, D. Walt, and S. Sonkusale, "Cmos microelectrode array for electrochemical lab-on-a-chip applications," *IEEE J. Sensors*, vol. 9, no. 6, pp. 609 –615, Jun. 2009.

[6] S. Bourcier, J.-F. Benoist, F. Clerc, O. Rigal, M. Taghi, and Y. Hoppilliard, "Detection of 28 neurotransmitters and related compounds in biological fluids by liquid chromatography/tandem mass spectrometry," *Rapid Communications in Mass Spectrometry*, vol. 20, no. 9, pp. 1405–1421, 2006. [Online]. Available: http://dx.doi.org/10.1002/rcm.2459

[7] T. Yao and G. Okano, "Simultaneous determination of l-glutamate, acetylcholine and dopamine in rat brain by a flow-injection biosensor system with microdialysis sampling," *Analytical Sciences*, vol. 24, no. 11, p. 1469, Sept. 2008.

[8] H. A. Pohl and K. Kaler, "Continuous dielectrophoretic separation of cell mixtures," *J. Cell Biochemistry and Biophysics*, vol. 1, no. 1, pp. 15–28, Mar 1979.

[9] M. Miled and M. Sawan, "Dielectrophoresis-based integrated lab-on-chip for nano and micro-particles manipulation and capacitive detection," *IEEE Trans. Biomed. Circuits. Syst.*, vol. 6, no. 2, pp. 120 –132, Apr. 2012.

[10] S. Westwood, S. Jaffer, O. Lui, and B. Gray, "Thick su-8 and pdms three-dimensional enclosed channels for free-standing polymer microfluidic systems," in *Proc. IEEE Canadian Conf. Elect. Comput. Eng. (CCECE)*, Apr. 2007, pp. 12 –15.

[11] S. Li and S. Chen, "Polydimethylsioxane fluidic interconnects for microfluidic systems," *IEEE Trans. Adv. Packag.*, vol. 26, no. 3, pp. 242–247, Aug. 2003.

[12] A. Pattekar and M. Kothare, "Novel microfluidic interconnectors for high temperature and pressure applications," *J. Micromech. Microeng.*, vol. 13, no. 2, pp. 337–345, Mar. 2003.

[13] E. Lee, D. Howard, E. Liang, S. Collins, and R. Smith, "Removable tubing interconnects for glass-based micro-fluidic systems made using ecdm," *J. Micromech. Microeng.*, vol. 14, no. 4, pp. 535 – 41, Apr. 2004.

[14] B. L. Gray, D. Jaeggi, N. J. Mourlas, B. P. van Drieënhuizen, K. R. Williams, N. I. Maluf, and G. T. A. Kovacs, "Novel interconnection technologies for integrated microfluidic systems," *J. Sensors and Actuators A: Physical*, vol. 77, no. 1, pp. 57 – 65, 1999.

[15] C. H. Kua, Y. C. Lam, C. Yang, K. Youcef-Toumi, and I. Rodriguez, "Modeling of dielectrophoretic force for moving dielectrophoresis electrodes," *J. Electrostatics*, vol. 66, no. 9-10, pp. 514 – 525, 2008.

[16] M. A. Miled, G. Massicotte, and M. Sawan, "Low-voltage lab-on-chip for micro and nanoparticles manipulation and detection: experimental results," *Analog Integrated Circuits and Signal Processing*, vol. 73, no. 3, pp. 1– 11, Dec. 2012.